ELSEVIER

Earth and Planetary Science Letters 203 (2002) 729–739

EPSL

www.elsevier.com/locate/epsl

Equation of state of gold and its application to the phase boundaries near 660 km depth in Earth's mantle

Sang-Heon Shim [a,*], Thomas S. Duffy [b], Takemura Kenichi [c]

[a] *Department of Earth and Planetary Science, University of California, Berkeley, CA 94720-4767, USA*
[b] *Department of Geosciences, Princeton University, Princeton, NJ 08544, USA*
[c] *National Institute for Materials Science, Namiki 1-1, Tsukuba, Ibaraki 305-0044, Japan*

Received 15 May 2002; received in revised form 10 July 2002; accepted 14 August 2002

Abstract

The pressure–volume–temperature equation of state (EOS) of gold is fundamental to high-pressure science because of its widespread use as an internal pressure standard. In particular, the EOS of gold has been used in recent in situ multi-anvil press studies for determination of phase boundaries related to the 660-km seismic discontinuity. These studies show that the boundaries are lower by 2 GPa than expected from the depth of the 660-km discontinuity. Here we report a new P–V–T EOS of gold based on the inversion of quasi-hydrostatic compression and shock wave data using the Mie–Grüneisen relation and the Birch–Murnaghan–Debye equation. The previously poorly constrained pressure derivative of isothermal bulk modulus and the volume dependence of Grüneisen parameter ($q = \mathrm{d}\ln\gamma/\mathrm{d}\ln V$) are determined by including both phonon and electron effects implicitly: $K'_{0T} = 5.0 \pm 0.2$ and $q = 1.0 \pm 0.1$. This combined with other accurately measured parameters enables us to calculate pressure at a given volume and temperature. At 660-km depth conditions, this new EOS yields 1.0 ± 0.2 GPa higher pressure than Anderson et al.'s EOS which has been used in the multi-anvil experiments. However, after the correction, there still exists a 1.5-GPa discrepancy between the post-spinel boundary measured by multi-anvil studies and the 660-km discontinuity. Other potential error sources, such as thermocouple emf dependence on pressure or systematic errors in spectroradiometry, should be investigated. Theoretical and experimental studies to better understand electronic and anharmonic effects in gold at high P–T are also needed.

Keywords: equations of state; gold; 660-km discontinuity; mantle

1. Introduction

Recent developments in multi-anvil press [1] and laser-heated diamond anvil cell [2,3] techniques together with synchrotron X-ray diffraction enable in situ determination of phase diagrams [1,4–9] and the equations of state of Earth materials [10,11] at deep interior conditions. These demand accurate in situ pressure calibrants whose equations of state are well known. The pressure-induced fluorescence shift of ruby [12] has been well established based on shock wave data for several metals. Recent independent calibration using Brillouin spectroscopy coupled with X-ray diffraction [13] confirms the accuracy of the

* Corresponding author. Tel.: +1-510-643-0540; Fax: +1-510-643-9980.
E-mail address: sangshim@uclink.berkeley.edu (S.-H. Shim).

0012-821X/02/$ – see front matter
PII: S0012-821X(02)00917-2

scale. The ruby scale is, however, not often used for in situ high-P–T studies for a variety of reasons, including the difficulty of separating pressure effects from temperature effects on the measured fluorescence shift.

For in situ X-ray diffraction studies, a pressure marker of known equation of state (EOS) is often used [14]. The criteria for choosing a suitable internal diffraction standard have been extensively discussed [15,16]. In general, gold is the material that best satisfies these criteria and thus it has been extensively used as an internal standard in both ambient- and high-temperature experiments in multi-anvil press. However, one disadvantage of gold is that existing equations of state [15,17–19] show significant discrepancies especially at high P–T. While most ultrasonic [20–23] and static compression [17,24] measurements generally agree on the bulk modulus, $K_{0T}=167$ GPa, its pressure derivative, K'_{0T}, is uncertain and spans a range from 5.0 [15] to 6.39 [20]. This results in about 10% uncertainty in the pressure determined from the gold EOS even at 300 K [16,25]. When fitting P–V–T experimental data to an EOS such as the Mie–Grüneisen–Debye model, even small errors in the reference isotherm at 300 K can lead to large systematic errors in the fit parameters (i.e., Grüneisen parameter) of the thermal EOS [26].

In recent studies using the gold scale, this uncertainty precludes determination of the phase boundaries in the MgO–SiO_2 system near 660 km depth with sufficient accuracy to test seismic and mineralogical models [1,5–8]. The conditions at 660 km depth (23–24 GPa and 1700–2000 K) require accurate determination of the thermal pressure because this quantity contributes 30–50% to the total pressure. Uncertainty in the pressure at 660 km depth is estimated to be $\sim$0.2 GPa based on comparison of different seismic and density models.

In this study, we constrain the pressure derivative of the bulk modulus, K'_{0T}, of gold from recent high-quality quasi-hydrostatic compression data measured at 300 K [27]. We then calculated the Grüneisen parameter at high P–T using this 300 K isotherm and Hugoniot data [28–32]. Our approach is similar to that of Heinz and Jeanloz [17]. However, in that study, the 300 K isotherm was obtained under non-hydrostatic conditions which are well-known to produce systematic error in the 300 K compression curve [33,34]. The data set used here was measured under negligible deviatoric stress using a helium pressure medium as discussed by Takemura [27]. We will compare this EOS with earlier studies [15,17,18] and apply this EOS for the recently measured phase boundaries in MgO–SiO_2 related to the 660-km seismic discontinuity.

2. Equation of state of gold

Takemura [27] recently reported the results of synchrotron X-ray diffraction experiments on gold samples contained within a helium or methanol pressure medium in a diamond anvil cell. The quasi-hydrostatic ruby fluorescence scale [12] was used for pressure determination over the range 0–75 GPa at 300 K in the helium experiment. Helium is well known to provide the most nearly hydrostatic pressure environment at pressures above 15 GPa [35]. That the stress distribution was in fact very close to hydrostatic was verified using several different criteria, including ruby peak widths and splittings, and X-ray diffraction peak width and lattice parameter variance from multiple diffraction lines. The latter approach should be an especially sensitive indicator of non-hydrostatic stresses in gold because of its large elastic anisotropy [33,34] and the demonstrated effects of non-hydrostatic stress on lattice parameter variance [34].

The P–V data of Takemura [27] with a helium medium were fitted to the third-order Birch–Murnaghan equation (Fig. 1):

$$P_{\mathrm{st}}(V)=\frac{3}{2}K_{0T}\left[\left(\frac{V_0}{V}\right)^{7/3}-\left(\frac{V_0}{V}\right)^{5/3}\right]\left\{1-\frac{3}{4}(4-K'_{0T})\left[\left(\frac{V_0}{V}\right)^{2/3}-1\right]\right\} \quad (1)$$

where P_{st} is the static pressure at 300 K, V is volume, and V_0 is the volume at 300 K and

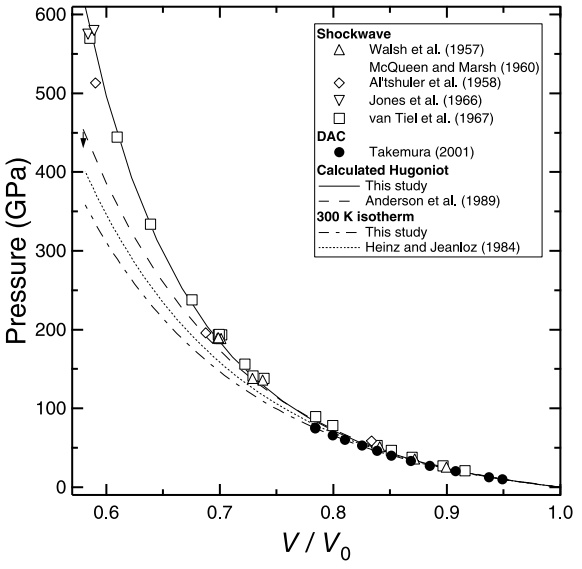

Fig. 1. Quasi-hydrostatic compression data at 300 K (solid circles [27]) and result of fit to 300 K isotherm (dash-dotted curve), and shock compression data (open up triangles [28,30]; open diamonds [29]; open down triangles [31]; open squares [32]) for gold. The 300 K isotherm measured by Heinz and Jeanloz [17] under non-hydrostatic conditions is shown for comparison (dotted curve). The Hugoniot calculated from equations of state by this study (solid curve) and Anderson et al. [18] (dashed curve) are shown. A vector represents the effect of anharmonic correction in Anderson et al.'s EOS.

1 bar. We performed two inversions: we fit K'_{0T} with fixed K_{0T} to 167 GPa from ultrasonic measurements [20–23] and we also fit both K_{0T} and K'_{0T} simultaneously. For each fit we assigned a weight to each data point based on the uncertainties of measured pressure and volume. We obtained $K'_{0T} = 5.01 \pm 0.02$ for the former inversion, and $K_{0T} = 164 \pm 1$ GPa and $K'_{0T} = 5.2 \pm 0.1$ for the latter inversion. Since the correlation between K_{0T} and K'_{0T} is known to be significant in a simultaneous fit of these parameters and the χ^2 of these two fits are almost identical, we prefer to use the former result. We take the difference between these two fitting results as a reasonable estimate for the uncertainties of the parameters: $\sigma(K_{0T}) =$ 3 GPa and $\sigma(K'_{0T}) = 0.2$.

The result of $K'_{0T} = 5.0$ is consistent with shock wave data [15], while this value is lower than all ultrasonic measurements, i.e., 5.21 [21] to 6.39 [20]. Duffy and Wang [16] compiled K_{0T} and K'_{0T} of metals measured by shock wave and ultrasonic, and found that ultrasonic measurements systematically overestimate K'_{0T} compared with shock wave values ($\sim$10%). They pointed out that significant variation of the value among ultrasonic measurement may imply that the values measured by ultrasonic technique available currently are not precise. In a recent refinement of the NaCl pressure scale, it was also recognized that lower-pressure measurements yield much higher K' than high-pressure measurements covering a wide pressure range [36]. In addition, K' of NaCl decreases rapidly below 3 GPa but decreases much more slowly at higher pressures. It should be noted that all the ultrasonic measurements for gold were conducted to maximum pressures of less than 1 GPa.

In the Mie–Grüneisen approach, pressure at a given volume and temperature, T, can be expressed as a sum of pressure along an isotherm, P_{st}, at a reference temperature, T_0 (= 300 K in this case), and an isochoric thermal pressure from the reference isotherm to the temperature of interest, $\Delta P_{th}(= P_{th}(V,T) - P_{th}(V,T_0))$:

$$P(V,T) = P_{st}(V,T_0) + \Delta P_{th}(V,T) \quad (2)$$

where P_{st} can be obtained from the 300 K isotherm (Eq. 1) and ΔP_{th} follows from the thermal energy, $\Delta E_{th}(V,T)$ ($= E_{th}(V,T) - E_{th}(V,T_0)$), as described in the Mie–Grüneisen equation:

$$\Delta P_{th}(V,T) = \frac{\gamma}{V}\Delta E_{th}(V,T) \quad (3)$$

where γ is the Grüneisen parameter.

The energy along the Hugoniot, E_H, is determined from the Rankine–Hugoniot equations to about 1% accuracy. To use this quantity, Eq. 3 can be rewritten as:

$$P_{st}(V,T_0) - P_H(V) = \frac{\gamma}{V}[E_{st}(V,T_0) - E_H(V)] \quad (4)$$

where P_H is the pressure along the Hugoniot. This enables us to calculate γ directly from the measured quantities, P_{st}, P_H, and $E_H - E_0$ for each

data point along the Hugoniot. However, it is necessary to know the 0 K isotherm to calculate E_{st}. We obtained the 0 K isotherm by subtracting $P_{th}(V,T_0)-P_{th}(V,0)$, obtained using Eq. 3 and the Debye model, from $P_{st}(V,T_0)$. In the Debye model, $E_{th}(V,T)$ can be calculated from:

$$E_{th}(V,T)=\frac{9nRT}{x^3}\int_0^x \frac{z^3}{(e^z-1)}\mathrm{d}z \quad (5)$$

where n is the number of atoms per formula unit, R is the gas constant, and $x=\theta(V)/T$ (θ is the Debye temperature). The volume dependence of θ is considered using:

$$\gamma=-\frac{\mathrm{d}\ln\theta}{\mathrm{d}\ln V} \quad (6)$$

If the Grüneisen parameter is expressed as a function of volume only, assuming q ($=\mathrm{d}\ln\gamma/\mathrm{d}\ln V$) is constant:

$$\gamma=\gamma_0\left(\frac{V}{V_0}\right)^q \quad (7)$$

the following relation can be obtained:

$$\theta=\theta_0\exp\left(\frac{\gamma_0-\gamma}{q}\right) \quad (8)$$

Once the 0 K isotherm is obtained, $E_{st}(V,300\ \mathrm{K})$ can be calculated by adding $E_{th}(V,T_0)$ (Eq. 5) to $E_{st}(V,0\ \mathrm{K})$ obtained from numerical integration of the 0 K isotherm. An important advantage of this approach is that γ is directly determined from high P–T data points. Furthermore, the assumption for the variation of γ (Eq. 7) is only used below 300 K where electronic and anharmonic effects are small, and thus this assumption does not influence the calculated γ values. This also allows inclusion of electronic and anharmonic contributions implicitly in the calculated γ. A similar approach can be found in the work by Hixson and Fritz [37], although they used this method for a forward calculation. An important difference in our approach is to restrict use of the phonon model, i.e., the Debye model, to temperatures below 300 K, where the overall electronic contribution is negligible and the phonon contribution is dominant.

We solved Eq. 4 numerically to calculate the Grüneisen parameter for each Hugoniot data point (Fig. 2a) and q using Eq. 7. It is observed that q converges to a constant value at high compression (Fig. 2b). Below 25% compression, the q

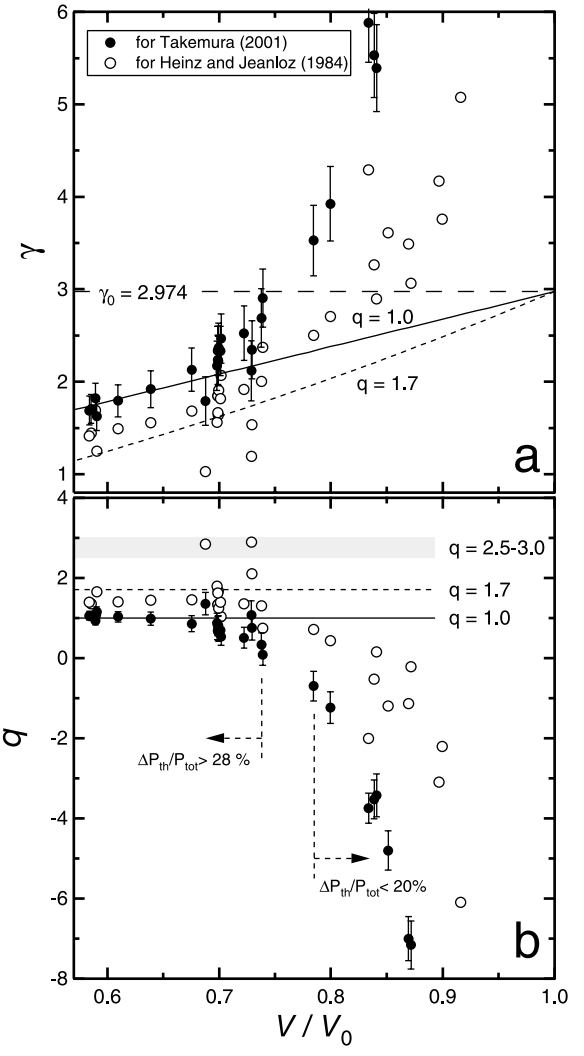

Fig. 2. Calculated (a) Grüneisen parameters, γ, and (b) their logarithmic volume derivatives, q, for Hugoniot data points using quasi-hydrostatic (solid circles [27]) and non-hydrostatic (open circles [17]) 300 K isotherms. Error bars (2σ) are calculated from the uncertainties of the 300 K isotherm and the Hugoniot. γ and q values obtained from this study (solid lines) and Heinz and Jeanloz [17] (dotted lines) are shown. The shaded area is the range of q values proposed by Anderson et al. [18]. Thermal pressure contribution to the total pressure, $\Delta P_{th}=P_{tot}$, is also indicated.

values are small and even negative. If correct, this implies that γ increases with compression which is unphysical (Fig. 2a). This may be understood as a result of a systematic trend caused by material strength which is significant at low compression (where temperatures are also low) along the Hugoniot [16,38,39]. In other words, the presence of shear strength along the Hugoniot results in a greater volume at lower pressure than expected for pure hydrodynamic compression. This greater volume requires a higher γ to explain the greater difference between the 300 K isotherm and the Hugoniot at a given pressure.

Also, the uncertainties of γ and q, which include both the uncertainties of the 300 K isotherm (uncertainties of both K_{0T} and K'_{0T}) and Hugoniot, decrease with compression. This is because γ and q at lower compression are extracted from the smaller difference between the 300 K isotherm and Hugoniot (i.e., thermal pressure). Thus, we select data points where the thermal pressure contribution is more than 28% ($P > 130$ GPa, $T > 2000$ K) and also where the shock temperature is high enough to relax shear stress. We calculated the average q for these data points by weighting with their thermal pressure contributions. q is calculated to be 1.00 ± 0.03. In order to test the robustness of this result, we also calculated q with different methods: weighting with ΔP_{th} for all data points ($q = 0.98 \pm 0.07$) and weighting with the estimated uncertainty for high-compression data points ($q = 0.89 \pm 0.03$). This shows that the uncertainty of q can be estimated to be ± 0.1.

In order to confirm consistency between this method and the approach by Heinz and Jeanloz [17], we also apply this method for their non-hydrostatic compression data. At high compression the calculated qs using this method lie at 1.7 ± 0.7 which is identical to those found in Heinz and Jeanloz [17] (Fig. 2b).

We performed another inversion following the approach by Hixson and Fritz [37]. We express Hugoniot pressure as a sum of static and thermal pressure using Eqs. 2 and 3:

$$P_H(V) = P_{st}(V, T_0) + \frac{\gamma}{V}\Delta E_{th}(V, T_H) \quad (9)$$

This equation requires to calculate temperature along the Hugoniot, T_H:

$$dT_H = -\gamma T\frac{dV}{V} + \frac{[(V_0 - V)dP_H + (P_H - P_0)dV}{2C_V} \quad (10)$$

where C_V is the isochoric heat capacity which can be calculated from the Debye model. Once T_H is known, ΔE_{th} can be obtained from the Debye model. We solved Eq. 9 numerically to calculate a q value for each Hugoniot data point by numerical integration of Eq. 10 using a Runge–Kutta routine with adaptive step size control [40]. Although this method only takes into account the phonon contributions, the result obtained from this approach is identical to the former approach within uncertainty.

Both anharmonic and electronic effects are significant at high temperatures, but they have opposite signs for gold [41]. If their magnitudes are comparable, these terms compensate each other and so deviation from the quasi-harmonic model may be negligible. The agreement between the above two approaches may imply that this may be the case for gold at high P–T. Nevertheless, further studies (e.g., [42]) are needed to better quantify the magnitude of these effects.

The q value obtained from the quasi-hydrostatic compression curve is significantly lower than the value obtained using the non-hydrostatic compression data [17]. However, our q value is consistent with those found for other metals from shock sound speed measurements [43] and static adiabatic compression measurements [44], where q values for many metals and other materials are observed to be close to 1.

It should be emphasized that the quasi-hydrostatic ruby scale [12] used for the static compression measurements is based in turn on the shock wave EOS of copper and silver. Thus, it is possible that the $q = 1$ assumption used for the reduction of the shock wave EOS influences the inverted value of q for gold. However, we note that the ruby scale is not based on any shock wave data for gold. Moreover, the accuracy of this ruby scale has recently been independently

Table 1
Thermodynamic parameters of gold

Parameter		References
V_0 (Å^3)	67.850 ± 0.004	[27]
K_{0T} (GPa)	167 ± 3	[20–23]
K'_{0T}	5.0 ± 0.2	This study
γ_0	2.97 ± 0.05	[18]
q	1.0 ± 0.1	This study
θ_0 (K)	170	[18]
$3nk$ (J/gK)	0.125	[15]
c_0 (km/s)	3.10 ± 0.02	This study
s	1.525 ± 0.008	This study

shown by a combined Brillouin and X-ray diffraction study [13].

A full set of parameters for the Birch–Murnaghan–Debye equation (Eqs. 1–3 and 5) is given in Table 1. We also present fitted parameters for the intercept, c_0, and the slope, s, of the linear particle velocity, U_P, and shock wave velocity, U_S, relation. Calculated pressures for given volumes and temperatures using our EOS are shown in Table 2.

In order to test our gold EOS, we calculate heat capacity, thermal expansion, and adiabatic bulk modulus, and compare with measured quantities at 1 bar and high temperatures [45–49]. We found good agreement in heat capacity for a wide range of temperature (0–1000 K) (Fig. 3a). Calculated thermal expansion parameters well match measured values below 600 K. At high temperature, our values are consistent with the lower values [47] among existing measurements (Fig. 3b). It should be noted that literature values for the thermal expansion of gold are discrepant by 10% at very high temperature (1000 K) [46]. In addition, anharmonic and electronic effects are significant in this high temperature range at 1 bar.

While calculated adiabatic bulk moduli are consistent with measurements [48,49] within uncertainty (2.5%), the temperature dependence of measured values ($\partial K_S/\partial T = -0.029$ GPa/K) is a factor of two smaller than that of calculated values (−0.014 GPa/K) (Fig. 3c). By transforming K_S to K_T and using:

$$\left(\frac{\partial(\alpha K_T)}{\partial V}\right)_T = -\frac{1}{V}\left(\frac{\partial K_T}{\partial T}\right)_V \tag{11}$$

it can be seen that the slope of Fig. 3c is related to anharmonicity (i.e., the volume dependence of thermal pressure, $P_{th} = \alpha K_T$) [18]. In fact, Anderson et al. [18] calculated the anharmonic correction based on this quantity. Using their procedure and the temperature dependence of K_T at 300 K

Table 2
Pressure (in GPa) at selected compressions and temperatures using the gold EOS from this study

$1-V/V_0$	300 K	500 K	1000 K	1500 K	2000 K	2500 K	3000 K
0.00	0.00	1.42	4.99	8.56	12.14	15.72	19.30
0.02	3.55	4.97	8.53	12.11	15.69	19.26	22.84
0.04	7.55	8.96	12.53	16.11	19.68	23.26	26.84
0.06	12.06	13.48	17.04	20.62	24.19	27.77	31.35
0.08	17.16	18.57	22.13	25.71	29.28	32.86	36.44
0.10	22.91	24.32	27.88	31.45	35.03	38.61	42.19
0.12	29.42	30.82	34.38	37.95	41.53	45.10	48.68
0.14	36.77	38.17	41.73	45.30	48.88	52.45	56.03
0.16	45.11	46.50	50.06	53.63	57.20	60.78	64.35
0.18	54.56	55.95	59.50	63.07	66.64	70.22	73.80
0.20	65.29	66.68	70.22	73.79	77.37	80.94	84.52
0.22	77.50	78.89	82.43	85.99	89.57	93.14	96.72
0.24	91.42	92.80	96.33	99.90	103.47	107.05	110.62
0.26	107.32	108.69	112.22	115.78	119.35	122.93	126.50
0.28	125.51	126.87	130.40	133.96	137.53	141.10	144.68
0.30	146.38	147.73	151.25	154.81	158.38	161.95	165.53
0.32	170.38	171.73	175.24	178.79	182.36	185.93	189.51
0.34	198.07	199.40	202.90	206.46	210.02	213.59	217.17

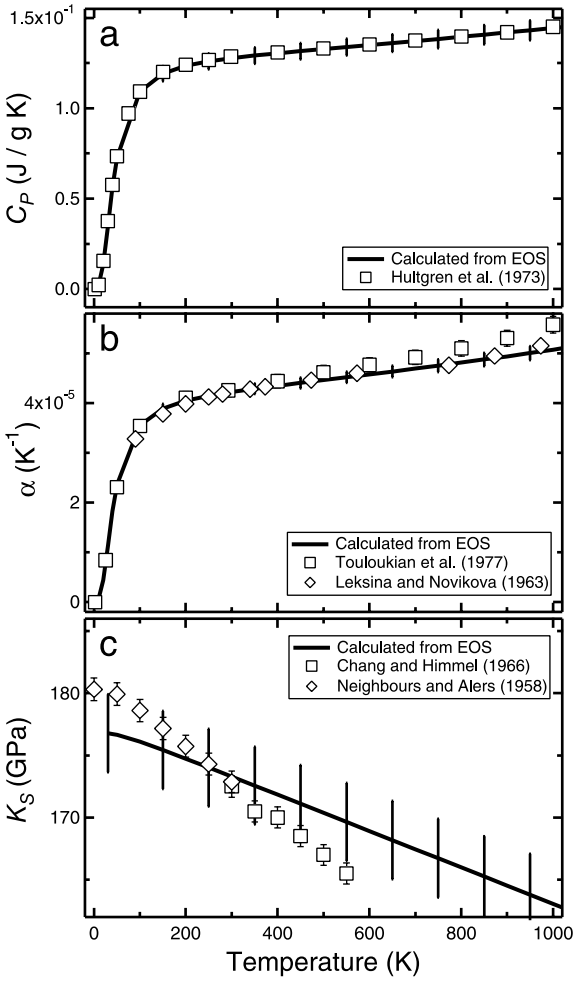

Fig. 3. Calculated (a) isobaric heat capacity, C_P, (b) thermal expansion, α, and (c) adiabatic bulk modulus of gold (solid lines) at ambient pressure and high temperature. Measured values are also plotted for comparison (open squares in a [45]; open squares in b [46], open diamonds in b [47]; open squares in c [48], open diamonds in c [49]). Error bars on the solid lines are the estimated uncertainty (1σ) calculated from the uncertainty of thermoelastic parameters in Table 1.

calculated from our EOS, we obtained $(\partial K_T/\partial T)_V = -0.7\times10^{-3}$ GPa/K, which is significantly smaller in magnitude than Anderson et al.'s value (-11.5×10^{-3} GPa/K). It should be noted that our value in Fig. 3c is calculated by projecting the EOS that is constrained by high P–T data to ambient pressure, whereas the ultrasonic measurements [48,49] were performed directly at ambient pressure. Thus, this discrepancy may imply that the volume dependence of thermal pressure, or anharmonicity, of gold is considerably suppressed at high P–T. In order to resolve the discrepancy in $\partial K_S/\partial T$ at 1 bar, one can calculate q just from 1 bar data, and then fix this, $q_0 = 2.5$–3.0, and introduce another functional form, such as $q = q_0(V/V_0)^{q_1}$, to describe the variation at high pressure [50]. For gold, however, there is no clear evidence that q follows such functional form at high pressure and in fact q is nearly constant as shown in Fig. 2b.

Uncertainty in pressure using our EOS can be calculated using the uncertainties of parameters listed in Table 1. For example, the pressure uncertainty at 660-km depth conditions (23–24 GPa and 1700–2000 K) is calculated to be 0.3 GPa. Another way to estimate the accuracy of our EOS is to check the uncertainty of the data set used to obtain it. The accuracy of the 300 K isotherm is mainly affected by the accuracy of ruby scale which is used for pressure measurement. The accuracy of ruby is estimated to be 1% [13]. In the course of data inversion, this propagates to a 0.2 GPa uncertainty for the 660-km depth conditions. Hugoniot data also have uncertainty. From the data scatter, the error from Hugoniot data may be 0.2 GPa at 660-km depth pressure. This means that the calculated uncertainty is a reasonable estimate of the accuracy of this EOS.

3. Comparison with previous studies and implication to the phase boundaries

In order to compare this EOS with previous studies [15,17,18], we plot pressure differences along selected isotherms (300, 1000, 2000, and 3000 K) (Fig. 4). Compared with this study, Jamieson et al.'s [15] EOS overestimates pressure below 130–160 GPa and underestimates beyond 130–160 GPa. They used the same Hugoniot data except the data by van Thiel et al. [32]. Although pressure and internal energy are well defined along the Hugoniot, in order to derive the EOS solely from Hugoniot data, one has to know γ_0 and q, and use a model to calculate the internal energy change. They assumed $\gamma_0 = 3.22$ instead of using a value calculated from accurate

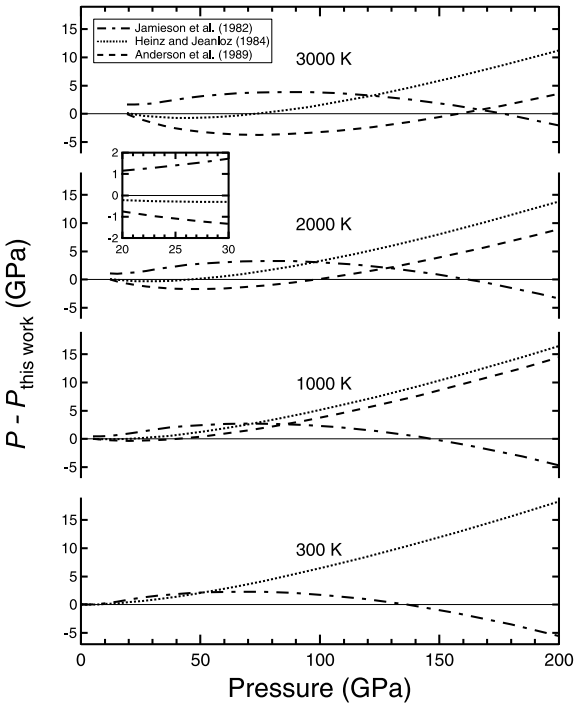

Fig. 4. Pressure differences calculated from the EOS of gold by this study (horizontal solid lines) with Jamieson et al. [15] (dash-dotted lines), Heinz and Jeanloz [17] (dotted lines), and Anderson et al. [18] (dashed lines) for 300, 1000, 2000, 3000 K isotherms. Anderson et al. [18] adapted the 300 K isotherm from Heinz and Jeanloz [17]. Pressure differences at 660-km depth conditions are shown in the inset.

room temperature measurements ($\gamma_0 = 2.97$). q was assumed to be 1.

Heinz and Jeanloz's [17] EOS overestimates pressure by 5% compared to our EOS at 300 K. Underestimation of pressure at moderate pressure (20–50 GPa) and high temperatures (2000 and 3000 K) is also notable. Using a forward calculation, they showed that the reduced 300 K isotherm from Hugoniot data using $\gamma_0 = 2.95 \pm 0.43$ and $q = 1.7 \pm 0.7$, both of which are calculated from measurements at ambient conditions, is consistent with their measured 300 K isotherm. However, their static measurement was performed with a methanol–ethanol pressure medium, which sustains significant shear stress above 10 GPa, and the q value is not directly determined from high-P–T data.

Anderson et al.'s [18] EOS underestimates pressure at low pressures and high temperatures. This becomes significant as temperature increases. They used non-hydrostatic compression measurements [17], and low- and high-temperature elasticity measurements at ambient pressure [48,49]. It is notable that this EOS is not tied to any high-P–T data. We calculated the Hugoniot using Anderson et al.'s EOS. Since the anharmonic correction in the EOS is not easily incorporated in Hugoniot calculation, we use $q = 2.5$–3.0, which was proposed by Anderson as a range consistent with his anharmonic EOS. This approach overestimated pressure by 4% compared with the original anharmonic EOS by Anderson as shown by the vector in Fig. 1, and thus this can be an upper bound for Anderson et al.'s EOS. As shown in Figs. 1 and 2, Anderson et al.'s EOS cannot match the shock wave data, which provide strong constraints on the thermal pressure. This limits the use of this EOS at high P–T conditions. In

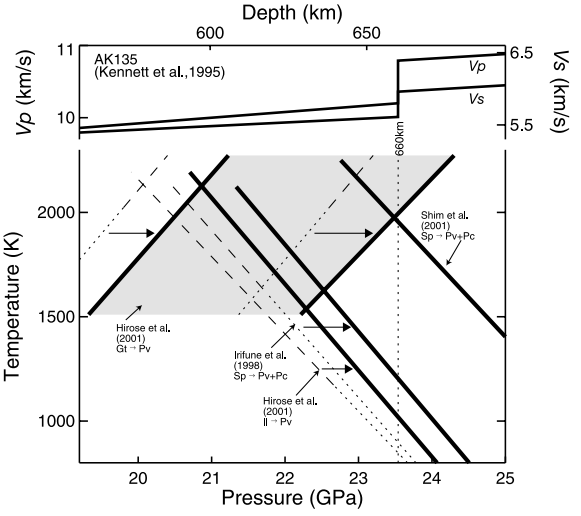

Fig. 5. Comparison between seismic velocity profiles (AK135 [56]) and experimental results (post-spinel [1,9]; post-ilmenite [7]; post-garnet [6]) at 550–700-km depth conditions. The phase boundaries measured using Anderson et al.'s [18] gold scale (dashed lines for the P–T conditions where measured and dotted lines for the P–T conditions where extrapolated) are corrected for the EOS of gold by this study (thick solid lines). The post-spinel boundary measured with platinum scale [9] is shown for comparison (Sp, spinel; Pv, perovskite; Pc, periclase; Il, ilmenite; Gt, garnet; V_P, P-wave velocity; V_S, S-wave velocity).

contrast, our EOS satisfies the shock wave data (Fig. 1).

The gold EOS by Holzapfel et al. [19] is obtained from shock wave and ultrasonic data using a modified pseudo-Debye–Einstein model and the EOS proposed by Holzapfel [51]. They used a much higher K'_{0T} (= 6.2) constrained by ultrasonic measurements performed to less than 1 GPa. At 1500 K and 25 GPa, we found that Holzapfel et al.'s EOS under-predicts pressure by 0.2 GPa compared with our EOS. Anderson et al.'s EOS under-predicts pressure by 0.6 GPa compared with Holzapfel et al.'s EOS at this condition.

Recent in situ determinations for the post-spinel [1], the post-ilmenite [5,7], and the post-garnet [6] phase transitions in the $MgO–SiO_2$ ($–Al_2O_3$) system were based on the gold scale by Anderson et al. [18]. However, more recent laser-heated diamond anvil cell studies [9,25] using ruby and platinum pressure scales reported that the post-spinel transition occurs close to 660-km depth condition.

We corrected the phase boundaries determined using Anderson et al.'s scale with our new gold scale (Fig. 5). At 660-km depth conditions (for T = 1800–2000 K), our EOS shifts the phase boundaries 1.0 GPa higher (the inset in Fig. 4). In addition, it slightly increases the slopes, although this increase is not significant considering the uncertainty. Even after the correction, however, the boundaries still yield unreasonably low temperatures at 660 km depth: 1200 K for the post-spinel and 1000 K for the post-ilmenite boundaries. The higher pressure phase boundary of the post-garnet reaction coincides with a plausible temperature at 660 km depth. However, considering that this transition occurs over a wider pressure range with a positive Clapeyron slope while seismic observations indicates that the 660-km discontinuity is much sharper with a negative slope [52], it is less likely that the post-garnet transition is the principal transition responsible for the 660-km seismic discontinuity.

Even with a 1.0 GPa correction to the gold scale, there still exists a 1.5 GPa discrepancy between the two in situ measurements [1,9] for the post-spinel boundary using different pressure scales. An important difference between these two in situ experiments involves the temperature measurements. Irifune et al. [1] used a thermocouple whereas Shim et al. [9] used radiometry. Since the thermocouple was placed in the pressure cell, the pressure effect on thermocouple emf should be considered. However, this effect is not well known and ignored. An experiment [53] at low pressure demonstrated that this effect may be significant: the order of 30 K at 5 GPa and 2000 K. To reconcile a 1.5 GPa discrepancy, the measured temperature would need to be in error by 200 K at 660-km depth conditions for the gold scale. However, significant issues associated with temperature measurement by spectroradiometry are also currently unresolved [54]. Further studies are needed to improve temperature measurements in both the diamond cell and large-volume press. Better understanding of electronic and anharmonic effects in gold are also needed.

4. Conclusion

The $P–V–T$ equation of state (EOS) of gold was determined by combining new quasi-hydrostatic compression data from a diamond anvil cell [27] and existing shock wave data [28–32]. From these data sets, the pressure derivative of the bulk modulus, K'_{0T}, is found to be 5.0 ± 0.2 and the logarithmic volume dependence of the Grüneisen parameter, q, is obtained to be 1.0 ± 0.1 from fitting to the Birch–Murnaghan and Grüneisen equations. Our data inversion implicitly includes the electronic contribution in the fitted Grüneisen parameter as well as the phonon contribution.

Our $P–V–T$ EOS shifts pressure by 1.0 GPa at 660-km depth conditions compared with Anderson et al.'s [18] EOS which was used in recent in situ multi-anvil determination of the phase boundaries [1,5,6] in the $MgO–SiO_2$ system near the 660-km seismic discontinuity. However, even after the correction, there remains 1.5 GPa discrepancy between these studies and the 660-km discontinuity. Other potential error sources, such as thermocouple emf dependence on pressure or systematic errors in spectroradiometry, should be investigated.

In addition to the phase boundary studies, the gold pressure scale has been used frequently in P–V–T measurements (e.g., $MgSiO_3$ perovskite [55]). Thus, it is expected that the fitted parameters, such as Grüneisen parameter and q, will be influenced by this pressure correction. A future study (Shim and Jeanloz, manuscript in preparation) will address this question.

Acknowledgements

This research was supported by the NSF. We are thankful for the discussion with K. Hirose, B. Anderson, and an anonymous reviewer. We also thank R. Jeanloz and D. Heinz for useful discussion. The Miller Institute is acknowledged for support to S.-H.S. *[BW]*

References

[1] T. Irifune, N. Nishiyama, K. Kuroda, T. Inoue, M. Isshiki, W. Utsumi, K.-I. Funakoshi, S. Urakawa, T. Uchida, T. Katsura, O. Ohtaka, The postspinel phase boundary in Mg_2SiO_4 determined by in situ X-ray diffraction, Science 279 (1998) 1698–1700.

[2] D. Andrault, G. Fiquet, Synchrotron radiation and laser heating in a diamond anvil cell, Rev. Sci. Instrum. 72 (2001) 1283–1288.

[3] G. Shen, M.L. Rivers, Y. Wang, S.R. Sutton, Laser heated diamond cell system at the Advanced Photon Source for in situ x-ray measurements at high pressure and temperature, Rev. Sci. Instrum. 72 (2001) 1273–1282.

[4] G. Shen, H.-K. Mao, R.J. Hemley, T.S. Duffy, M.L. Rivers, Melting and crystal structure of iron at high pressures and temperatures, Geophys. Res. Lett. 25 (1998) 373–377.

[5] K. Kuroda, T. Irifune, N. Nishiyama, M. Miyashita, K.-I. Funakoshi, W. Utsumi, Determination of the phase boundary between ilmenite and perovskite in $MgSiO_3$ by in situ X-ray diffraction and quench experiments, Phys. Chem. Mineral. 27 (2000) 523–532.

[6] K. Hirose, Y. Fei, S. Ono, T. Yagi, K.-I. Funakoshi, *In situ* measurements of the phase transition boundary in $Mg_3Al_2Si_3O_{12}$: implications for the nature of the seismic discontinuities in the Earth's mantle, Earth Planet. Sci. Lett. 184 (2001) 567–573.

[7] K. Hirose, T. Komabayashi, M. Murakami, K.-I. Funakoshi, *In situ* measurements of the majorite-akimotoite-perovskite phase transition boundaries in $MgSiO_3$, Geophys. Res. Lett. 22 (2001) 4351–4354.

[8] S. Ono, T. Katsura, E. Ito, M. Kanzaki, A. Yoneda, M.J. Walter, S. Urakawa, W. Utsumi, K. Funakoshi, In situ observation of ilmenite-perovskite phase transition in $MgSiO_3$ using synchrotron radiation, Geophys. Res. Lett. 28 (2001) 835–838.

[9] S.-H. Shim, T.S. Duffy, G. Shen, The post-spinel transformation in Mg_2SiO_4 and its relation to the 660-km seismic discontinuity, Nature 411 (2001) 571–574.

[10] G. Fiquet, A. Dewaele, D. Andrault, M. Kunz, T. Le-Bihan, Thermoelastic properties and crystal structure of $MgSiO_3$ perovskite at lower mantle pressure and temperature conditions, Geophys. Res. Lett. 27 (2000) 21–24.

[11] S.-H. Shim, T.S. Duffy, G. Shen, The stability and P-V-T equation of state for $CaSiO_3$ perovskite in the earth's lower mantle, J. Geophys. Res. 105 (2000) 25955–25968.

[12] H.-K. Mao, J. Xu, P.M. Bell, Calibration of the ruby pressure gauge to 800 kbar under quasihydrostatic conditions, J. Geophys. Res. 91 (1986) 4673–4676.

[13] C.S. Zha, H.-K. Mao, R.J. Hemley, Elasticity of MgO and a primary pressure scale to 55 GPa, Proc. Natl. Acad. Sci. USA 97 (2000) 13494–13499.

[14] R. Miletich, D.R. Allan, W.F. Kuhs. High-pressure single-crystal techniques, in: R.M. Hazen, R.T. Downs (Eds.), High-Temperature and High-Pressure Crystal Chemistry, Mineralogical Society of America, 2000, pp. 445–519.

[15] J.C. Jamieson, J.N. Fritz, M.H. Manghnani. Pressure measurement at high temperature in X-ray diffraction studies: gold as a primary standard, in: S. Akimoto, M.H. Manghnani (Eds.), High-Pressure Research in Geophysics, Center for Academic Publications Japan, Tokyo, 1982, pp. 27–48.

[16] T.S. Duffy, Y. Wang. Pressure-volume-temperature equations of state, in: R.J. Hemley (Ed.), Ultrahigh-Pressure Mineralogy, Rev. Mineral. 37 (1998) 425–457.

[17] D.L. Heinz, R. Jeanloz, The equation of state of the gold calibration standard, J. Appl. Phys. 55 (1984) 885–893.

[18] O.L. Anderson, D.G. Isaak, S. Yamamoto, Anharmonicity and the equation of state for gold, J. Appl. Phys. 65 (1989) 1534–1543.

[19] W.B. Holzapfel, M. Hartwig, W. Sievers, Equations of state for Cu, Ag, and Au for wide ranges in temperature and pressure up to 500 GPa and above, J. Phys. Chem. Ref. Data 30 (2001) 515–529.

[20] W.B. Daniels, C.S. Smith, Pressure derivatives of the elastic constants of copper, silver, and gold to 10,000 bars, Phys. Rev. 111 (1958) 713–721.

[21] Y. Hiki, A. Granato, Anharmonicity in noble metals; higher order elastic constants, Phys. Rev. 144 (1966) 411–419.

[22] B. Golding, S.C. Moss, B.L. Averbach, Composition and pressure dependence of the elastic constants of gold-nickel alloys, Phys. Rev. 158 (1967) 637–646.

[23] S.N. Biswas, P. Van 't Klooster, N.J. Trappeniers, Effect of pressure on the elastic-constants of noble-metals from 196°C to +25°C and up to 2500 bar. 2. Silver and gold, Physica B 103 (1981) 235–246.

[24] L.C. Ming, D. Xiong, M.H. Manghnani, Isothermal com-

pressionn of Au and Al to 20 GPa, Physica 139 (1986) 174–176.
[25] L. Chundinovskikh, R. Boehler, High-pressure polymorphs of olivine and the 660-km seismic discontinuity, Nature 411 (2001) 574–577.
[26] S.-H. Shim, T.S. Duffy, Constraints on the P-V-T equation of state of $MgSiO_3$ perovskite, Am. Mineral. 85 (2000) 354–363.
[27] K. Takemura, Evaluation of the hydrostaticity of a helium-pressure medium with powder x-ray diffraction techniques, J. Appl. Phys. 89 (2001) 662–668.
[28] J.M. Walsh, M.H. Rice, R.G. McQueen, F.L. Yarger, Shock-wave compressions of twenty-seven metals, equation of state of metals, Phys. Rev. 108 (1957) 196–216.
[29] L.V. Al'tshuler, K.K. Krupnikov, M.I. Brazhnik, Dynamic compressibility of metals under pressures from 400,000 to 4,000,000 atmospheres, Sov. Phys. JETP 34 (1958) 614–619.
[30] R.G. McQueen, S.P. Marsh, Equation of state of nineteen metallic elements from shock-wave measurements to two megabars, J. Appl. Phys. 31 (1960) 1253–1269.
[31] A.H. Jones, W.M. Isbell, C.J. Maiden, Measurement of the very-high-pressure properties of materials using a light-gas gun, J. Appl. Phys. 37 (1966) 3493–3499.
[32] M. van Thiel, A.S. Kusubov, A.C. Mitchell. Compendium of shock wave data, Technical Report UCRL-50108, Lawrence Radiation Laboratory, Livermore, CA, 1967.
[33] Y. Meng, D.J. Weidner, Y. Fei, Deviatoric stress in a quasi-hydrostatic diamond anvil cell: Effect on the volume-based pressure calibration, Geophys. Res. Lett. 20 (1993) 1147–1150.
[34] T.S. Duffy, G. Shen, D.L. Heinz, A.K. Singh, Lattice strains in gold and rhenium under non-hydrostatic compression to 37 GPa, Phys. Rev. B Condens. Matter 60 (1999) 15063–15073.
[35] H.K. Mao, R.J. Hemley, Y. Wu, A.P. Jephcoat, L.W. Finger, C.S. Zha, W.A. Bassett, High-pressure phase diagram and equation of state of solid helium from single-crystal X-ray diffraction to 23.3 GPa, Phys. Rev. Lett. 60 (1988) 2649–2652.
[36] J.M. Brown, The NaCl pressure standard, J. Appl. Phys. 86 (1999) 5801–5808.
[37] R.S. Hixson, J.N. Fritz, Shock compression of tungsten and molybdenum, J. Appl. Phys. 71 (1992) 1721–1728.
[38] R.G. McQueen, S.P. Marsh, J.W. Taylor, J.N. Fritz, W.J. Carter. The equation of state of solids from shock wave studies, in: R. Kinslow (Ed.), High Velocity Impact Phenomena, Academic Press, New York, 1970, pp. 293–417.
[39] J.R. Asay, The use of shock-structure methods for evaluating high-pressure material properties, Int. J. Impact Eng. 20 (1997) 27–61.
[40] W.H. Press, B.P. Flannery, S.A. Teukolsky, W.T. Wetterling. Numerical Recipes in C – The Art of Scientific Computing, Cambridge University Press, Cambridge, 1988.
[41] D.C. Wallace. Thermodynamics of Crystals, Wiley, New York, 1972.
[42] M. Okube, A. Yoshiasa, O. Ohtaka, H. Fukui, Y. Katayama, W. Utsumi, Anharmonicity of gold under high-pressure and high-temperature, Solid State Commun. 121 (2002) 235–239.
[43] T.S. Duffy, T.J. Ahrens. Hugoniot sound velocities in metals with applications to the earth's inner core, in: Y. Syono, M.H. Manghnani (Eds.), High-Pressure Research: Application to Earth and Planetary Sciences, Terra Scientific, 1992, pp. 353–361.
[44] R. Boehler, J. Ramakrishnan, Experimental results on the pressure dependence of the Grüneisen parameter: A review, J. Geophys. Res. 85 (1980) 6996–7002.
[45] R. Hultgren, P.D. Desai, D.T. Hawkins, M. Gleiser, K.K. Kelley (Eds.). Selected Values of the Thermodynamic Properties of the Elements, American Society for Metals, Metals Park, OH, 1973.
[46] Y.S. Touloukian, R.K. Kirby, R.E. Taylor, P.D. Desai. Thermal Expansion – Metallic Elements and Alloys, volume 12 of Thermophysical Properties of Matter, Plenum, New York, 1977.
[47] I.E. Leksina, S.I. Novikova, Thermal expansion of copper, silver, and gold within a wide range of temperatures, Sov. Phys. – Solid State 5 (1963) 798–801.
[48] Y.A. Chang, L. Himmel, Temperature dependence of elastic constants of Cu, Ag, and Au above room temperature, J. Appl. Phys. 37 (1966) 3567–3567.
[49] J.R. Neighbours, G.A. Alers, Elastic constants of silver and gold, Phys. Rev. 111 (1958) 707–712.
[50] S. Speziale, C.-S. Zha, T.S. Duffy, R.J. Hemley, H.-K. Mao, Quasi-hydrostatic compression of magnesium oxide to 52 GPa: implications for the pressure-volume-temperature equations of state, J. Geophys. Res. 106 (2001) 515–528.
[51] W.B. Holzapfel, Equations of state for solids under strong compression, High Pressure Res. 16 (1998) 81–126.
[52] S. Lebedev, S. Chevrot, R. VanderHilst, Seismic evidence for olivine phase changes at the 410- and 660-kilometer discontinuities, Science 296 (2002) 1300–1302.
[53] I.C. Getting, G.C. Kennedy, Effect of pressure on the emf of chromel-alumel and platinum-platinum 10% rhodium thermocouples, J. Appl. Phys. 41 (1970) 4552–4562.
[54] A.P. Jephcoat, S.P. Besedin, Temperature measurement and melting determination in the laser-heated diamond-anvil cell, Phil. Trans. R. Soc. London A 354 (1996) 1333–1360.
[55] N. Funamori, T. Yagi, W. Utsumi, T. Kondo, T. Uchida, Thermoelastic properties of $MgSiO_3$ perovskite determined by in situ X-ray observations up to 30 GPa and 2000 K, J. Geophys. Res. 101 (1996) 8257–8269.
[56] B.L.N. Kennett, E.R. Engdahl, R. Buland, Constraints on seismic velocities in the Earth from travel times, Geophys. J. Int. 122 (1995) 108–124.